Label-free biomolecular imaging using scanning spectral interferometry

Tongzhou Wang (王同舟)[1†], Liping Xie (谢丽萍)[1†], Haley Huang[2], Xin Li (黎 新)[1], Ruliang Wang (汪汝亮)[1], Guang Yang (杨 光)[1], Yanan Du (杜亚楠)[1*], and Guoliang Huang (黄国亮)[1,3]**

[1]*Department of Biomedical Engineering, Tsinghua University School of Medicine, Beijing 100084, China*

[2]*Department of Biomedical Engineering, Johns Hopkins University, Baltimore, MD 21287, USA*

[3]*National Engineering Research Center for Beijing Biochip Technology, Beijing 102206, China*

[*]*Corresponding author: duyanan@tsinghua.edu.cn;* [**]*corresponding author: tshgl@tsinghua.edu.cn*

[†]*These authors contributed equally to this work*

Received July 16, 2013; accepted October 17, 2013; posted online November 9, 2013

This letter presents a label-free biomolecular imaging technique based on white-light interferometry and spectral detection. The method measures thickness changes caused by specific binding between biomolecules to detect the presence of certain analyte. A spectrum-shifting algorithm is developed to resolve the thickness information from the spectrum. The axial resolution of the experimental instrument can reach ∼1 nm, thereby enabling detection of trace amounts (∼1 ng/mm^2) of proteins or DNA. This letter also presents two experiments to prove the feasibility of the method for detecting proteins and DNA without fluorescent labeling.

OCIS codes: 110.0110, 120.0120, 300.0300, 330.0330.

doi: 10.3788/COL201311.111102.

Developments in optical microscope technology have achieved remarkable progress from the 1980s to the last decade. The detection resolution of technologies such as stimulated emission depletion (STED)[1−3], PALM[4], and STORM[5], has reached scales as low as tens of nanometers. All of the technologies developed thus far use fluorescent labels to improve their resolution; however, these fluorescent dyes present negative effects on life activities[6]. Fluorescent labels also undergo photobleaching, which further complicates the analysis of experimental results.

Important progress in label-free detection methods, such as surface plasmon resonance (SPR)[7,8], microresonators[9], interferometry[10,11], and electrochemistry[12], has been achieved. Among these methods, interferometry is one of the most convenient and widely applicable technologies for measuring small changes in biochemical reactions[13].

Unfortunately, because most label-free detection methods are indirect, which means the biochemical signal is converted to another type of signal, introduction of errors to the results is unavoidable. Because of this issue, many researchers still regard molecular images as the most reliable evidence of biochemical reactions. SPR imaging (SPRI)[14,15] devices based on the traditional SPR device, which produces an image that describes energy absorption in a two-dimensional (2D) field, may be used for sample imaging. Similar to SPR technology, however, SPRI requires an expensive gold-coated chip, which raises the cost of detection.

Interferometry, another promising method for label-free molecular imaging, presents advantages of convenience, low cost, and high sensitivity. Previous studies[13,16−19] on interferometry detection report that the spectrum of the reflected light beam can be used to measure the presence of biomolecules. Thus, interferometry is a novel method for detecting trace amounts of biomolecules without fluorescent labelling. Many devices, including spectral reflectance imaging biosensors[13] and interferometric reflectance imaging sensors[19], have been designed to achieve label-free biomolecular detection. These devices use phase shifts ($\Delta\Phi$) to evaluate thickness changes introduced by biomolecular binding because interferometric measurements are extremely sensitive to phase change (10^{-10} rad)[18]. However, $\Delta\Phi$ does not show a linear relationship with the thickness increment. As such, the overall $\Delta\Phi$ cannot represent the average thickness increment of a detection area if the thickness increment within the area is inconsistent. This limitation presents difficulties in high-resolution imaging because the thickness increment within the area of a pixel does not have a linear relationship with its gray values in the resulting images. Thus, common post-processing methods for reconstructing high-resolution images, such as deconvolution and 2D Fourier transformation, are inapplicable.

This letter presents a scanning-probe-style interferometric super-resolution microscope that can capture high-resolution molecular images without fluorescent labelling. A novel algorithm is introduced to extract a linear relationship between the thickness increment and the image gray value. The algorithm used in our experiment provides better linearity compared with the phase-resolving algorithm used in the majority of other studies[18,19]. Good linearity is extremely important in scanning-probe-style microscopes because the device requires deconvolution to cancel the artifacts introduced by pixel overlapping.

The setup of the microscope is demonstrated in Fig. 1(a). The structure is similar to a Michelson interferometer, except for the coaxial measurement and reference arms. The sample is attached to a SiO_2-coated silicon chip and illuminated by a wide-band light source, such as a halogen tungsten or deuterium lamp. Figure 1(b)

 © 2013 Chinese Optics Letters

shows that two reflections form when the beam reaches the chip and are positioned as follows: one on top of the biomolecular layer or top of the SiO_2 film if no probes are present on that spot (corresponding to "reflected beam 1") and the other on the surface of the silicon base (corresponding to "reflected beam 2"). When the two reflected beams recombine, they interfere and produce a stable spectral pattern that contains information on their optical length difference. The recombined beam is then reflected by the beam splitter, passes through a converging lens and an aperture, and is finally collected by a fiber connected to a spectrometer. A piezo-driven stage (P-915K585, Physik Instrumente, Germany) with 2-nm xy resolution is installed under the chip to provide high lateral resolution.

The microscope analyzes the spectrum of the recombined reflecting beam to calculate the thickness increment of the biomolecular layer. When an analyte is caught by a probe, the biomolecular layer thickens such that the optical length difference between the two reflected light beams also increases. This optical length difference increment results in red-shifting in the reflective spectrum (Fig. 2). Changes in thickness can be

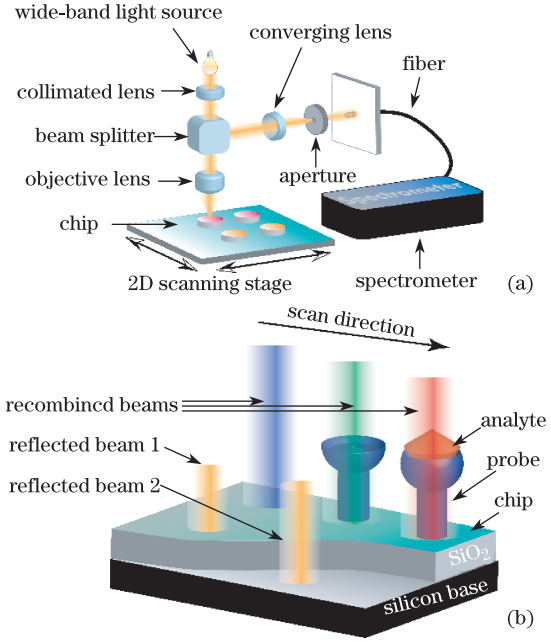

Fig. 1. (Color online) Setup of the scanning interferometric super-resolution microscope.

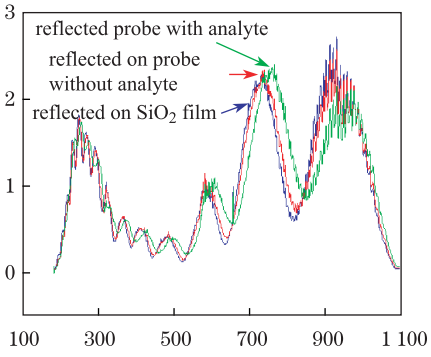

Fig. 2. (Color online) Reflective spectrum of the recombined beams.

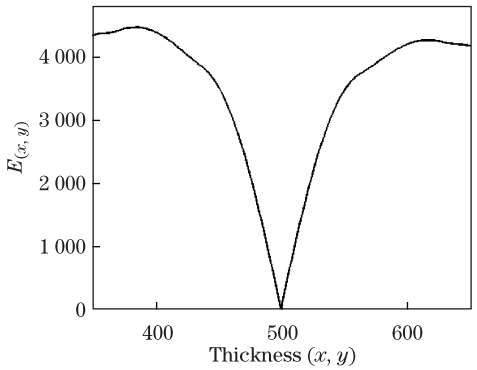

Fig. 3. Relationship between $E_{x,y}$ and thickness (thickness of the reference point=500 nm).

calculated by quantifying the red-shifting in the spectrum.

We firstly select a point on the detecting surface and define its altitude as 0 to quantify the red-shifting. Then, the reflective spectrum of that point is collected by the spectrometer and later used as the "reference spectrum" ($S_{\text{reference}}(\lambda)$). During the imaging process, the spectrum of every point ($S_{x,y}(\lambda)$) is subtracted by the reference spectrum, which generates a 2D image of differential spectra ($D_{x,y}(\lambda)$). This relationship can be expressed as

$$D_{x,y}(\lambda) = S_{x,y}(\lambda) - S_{\text{reference}}(\lambda). \tag{1}$$

The differential spectra are accumulated within the spectral detection ranges, thereby generating an equivalent scalar value (E) representing the thickness variation; this value can be expressed as

$$E_{x,y} = \int |D_{x,y}(\lambda)| \cdot \mathrm{d}\lambda. \tag{2}$$

A simulation is performed to evaluate the relationship between $E_{x,y}$ and thickness changes. The result is shown in Fig. 3.

Figure 3 indicates that the overall thickness of the SiO_2 film and biomolecular layer has a linear relationship with $E_{x,y}$ if the thickness difference relative to the reference point is no larger than 50 nm. However, the slope between $E_{x,y}$ and thickness varies with the spectrum of the illuminating light and the transparency of the film. We measured the $E_{x,y}$ of a photo-etched Si-SiO_2 chip illuminated by a halogen tungsten lamp to achieve a slope of 2.0873×10^4 nm^{-1} and a standard division (δ) of dark noise of 7133.82. In this case, the limit of detection (LOD) can be calculated as

$$\text{LOD} = \frac{3\delta}{\text{slope}} = \frac{3 \times 7133.82}{20873/\text{nm}} \approx 1.0 \text{ nm}. \tag{3}$$

Thus, the proposed device can detect trace amounts of proteins or DNA with ~1 nm axial resolution. The size of an IgG protein molecule ranges from 5 to 10 nm, and the distance between two bases in DNA is 0.34 nm. Thus, a resolution of about 1 nm is adequate for single-molecule-layer detection.

The proposed device can be used to detect the specific binding of biomolecules without fluorescent labeling. Here, an antibody-detection experiment was conducted to verify the feasibility of the device (Fig. 4).

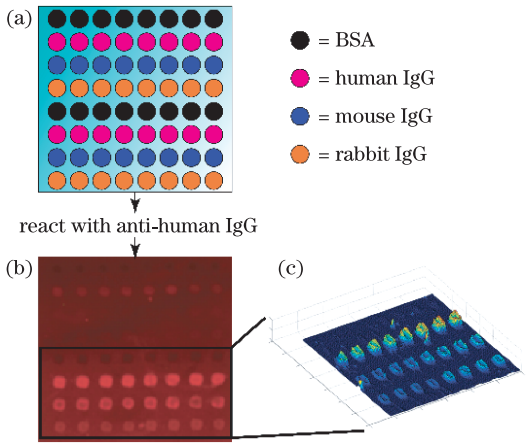

Fig. 4. (Color online) Detection of antibodies using the proposed interferometric super-resolution microscope.

In this experiment, a SiO_2-coated silicon chip was immersed in 3-glycidyloxypropyl trimethoxysilane (CAS:2530-83-8) for 28 h at 55 °C[20] to achieve epoxy modification and provide extra affinity between the SiO_2 film and protein molecules. Then, four proteins, i.e., bovine serum albumin (BSA), human IgG, mouse IgG, and rabbit IgG, were attached to the chip by SmartArrayer (CapitalBio, China). Each protein was prepared at two concentrations (1 and 5 mg/mL), and each concentration was applied in eight sample spots to form an 8×8 microarray chip (Fig. 4(a)). The chip was then incubated with anti-human IgG with Cy-3 fluorescent labels for 30 min at 37 °C. Anti-human IgG binds specifically to human IgG and not to BSA, mouse IgG, or rabbit IgG. Therefore, the probe spots in the 2nd and 6th rows of the chip emit stronger fluorescence signals than the other rows (Fig. 4(b)). The same chip was then scanned by the proposed interferometric super-resolution microscope to obtain the surface profile of the four lower rows. The results (Fig. 4(c)) prove that the fluorescence of probes on the 6th row of the chip is greater than that in the other rows, which is consistent with the results of fluorescent labeling (Fig. 4(b)).

The specificity of the proposed detection method is demonstrated. As shown in Fig. 5, two 5×12 microarray chips were constructed to carry four types of probes (i.e., human IgG, mouse IgG, rabbit IgG, and goat IgG). As probe concentrations also affect the amount of analyte being detected, three probe concentrations (5, 2.5, and 1.25 mg/mL) were used for each probe. Probes with higher concentrations could extend the limit of detection but may also introduce false-positive signals if the analyte is excessively concentrated. Conversely, probes with lower concentrations may be unable to detect diluted samples but would be less affected by non-specific bindings. Chips featuring multiple concentrations of probes are thus more adaptable to common sampling procedures than chips with limited concentrations of probes.

Serum samples were obtained from goat peripheral blood without purification to simulate a clinical testing scenario. Two samples of serum with titer=1:32 were incubated with the chips. One sample contained anti-human IgG while the other contained anti-mouse IgG.

The chips were incubated with the samples for 30 min at 37 °C, washed, and dried for detection. Figure 5 shows an image obtained from the experimental interferometric super-resolution microscope. Figure 5(a) shows an image of the chip incubated with anti-human IgG. The first three rows on the chip, which contain human IgG as probes, are thicker than the other rows. By contrast, the 4th–6th rows in Fig. 5(b), which contain anti-mouse IgG, are thicker than other rows when the chip is incubated with anti-mouse IgG.

The microscope can also be used to observe DNA amplicons without fluorescence labeling, as confirmed by another experiment. Briefly, a 3×5 (mm) silicon chip with amine-modified SiO_2 film on its surface was spotted with three DNA primers (positive control, analyte, and negative control; Fig. 6(a)). All of the primers had a concentration of 10 μmol/L. Then, a single-stranded DNA template was added to the chip. After 30 min of incubation at 60 °C and another 30 min of incubation at 25 °C, the template could bind to certain DNA sequences of the primers (Fig. 6(d)). About 5 μL of ligation mixture containing T4 enzyme was subsequently added to each microarray of the chip, and the chip was incubated at 25 °C for 4 h. This procedure connects the two ends of the templates (Fig. 6(e)), thereby forming a circular template for the following rolling cycle amplification (RCA). The ligation mixture was washed off, and 5 μL of RCA reaction solution containing Phi 29 DNA polymerase was added to each microarray in the chip. The chip was then

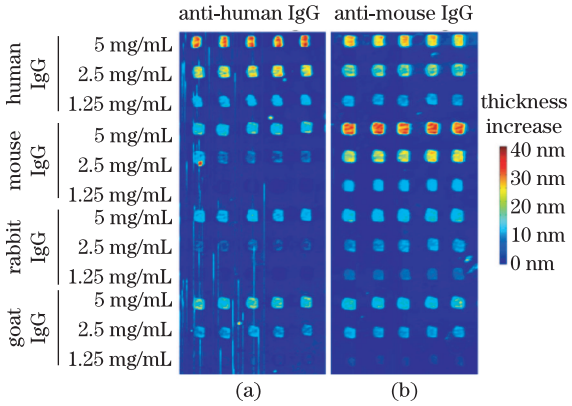

Fig. 5. (Color online) Serum sample testing with anti-human IgG and anti-mouse IgG.

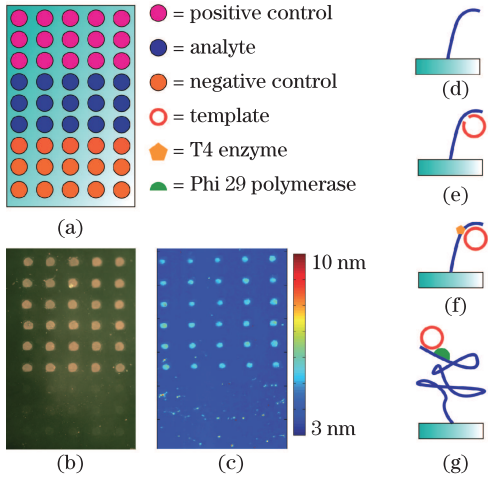

Fig. 6. (Color online) Observation of DNA amplicon by scanning interferometric microscope.

incubated at 30 °C for 16 h, during which the Phi 29 DNA polymerase extends the primers by replicating the circular template (Fig. 6(f)). Finally, the chip was washed, dried, and scanned by the interferometric microscope. Figure 6(c) shows that the thickness of the DNA amplicon is < 10 nm but could still observed clearly by the proposed microscope. A SYBR Green II fluorescence-labeled image captured for comparison is shown in Fig. 6(b). The results between Figs. 6(b) and (c) are identical.

In conclusion, the scanning interferometric microscope reported in this letter features a 1-nm axial resolution and can thus be used to observe small thickness changes brought about by biomolecular bindings. Experiments prove that biomolecules, including proteins and DNA, can be clearly observed by our microscope. This instrument presents a novel and promising method for molecular imaging and may be extremely useful in biochemical studies.

This work was supported by the National Supporting Plan of China (No. 2012BAI23B01), the National Natural Science Foundation of China (No. 81327005), the National "973" Program of China (No. 2011CB707701), the National Foundation of High Technology of China (Nos. 2012AA020102 and 2013AA041201), and the Biomedical Detection Technology and Instrument Laboratory of Beijing Foundation.

References

1. S. W. Hell and J. Wichmann, Opt. Lett. **19,** 780 (1994).
2. G. Vicidomini, G. Moneron, K. Y. Han, V. Westphal, H. Ta, M. Reuss, J. Engelhardt, C. Eggeling, and S. W. Hell, Nat. Methods **8,** 571 (2011).
3. Y. Chen, H. Guo, W. Gong, L. Qin, H. Aleyasin, R. R. Ratan, S. Cho, J. Chen, and S. Xie, Chin. Opt. Lett. **11,** 011703 (2013).
4. S. T. Hess, T. P. Girirajan, and M. D. Mason, Biophys. J. **91,** 4258 (2006).
5. M. J. Rust, M. Bates, and X. Zhuang, Nat. Methods **3,** 793 (2006).
6. B. N. Giepmans, S. R. Adams, M. H. Ellisman, and R. Y. Tsien, Science **312,** 217 (2006).
7. J. M. Bingham, J. N. Anker, L. E. Kreno, and R. P. Van Duyne, J. Am. Chem. Soc. **132,** 17358 (2010).
8. X. Chen, L. Liu, Z. Liu, H. Shi, S. Ma, Y. He, and J. Guo, Chin. Opt. Lett. **10,** S12401 (2012).
9. D. X. Xu, M. Vachon, A. Densmore, R. Ma, A. Delage, S. Janz, J. Lapointe, Y. Li, G. Lopinski, D. Zhang, Q. Y. Liu, P. Cheben, and J. H. Schmid, Opt. Lett. **35,** 2771 (2010).
10. A. Kussrow, C. S. Enders, and D. J. Bornhop, Anal. Chem. **84,** 779 (2012).
11. J. Zheng, B. Yao, R. A. Rupp, T. Ye, P. Gao, J. Min, and R. Guo, Chin. Opt. Lett. **10,** 010901 (2012).
12. D. Xu, D. Xu, X. Yu, Z. Liu, W. He, and Z. Ma, Anal. Chem. **77,** 5107 (2005).
13. E. Ozkumur, J. W. Needham, D. A. Bergstein, R. Gonzalez, M. Cabodi, J. M. Gershoni, B. B. Goldberg, and M. S. Unlu, Proc. Natl. Acad. Sci. Unit. States Am. **105,** 7988 (2008).
14. S. Chen, T. Deng, T. Wang, J. Wang, X. Li, Q. Li, and G. Huang, J. Biomed. Opt. **17,** 015005 (2012).
15. P. Guedon, T. Livache, F. Martin, F. Lesbre, A. Roget, G. Bidan, and Y. Levy, Anal. Chem. **72,** 6003 (2000).
16. E. Ozkumur, S. Ahn, A. Yalcin, C. A. Lopez, E. Cevik, R. J. Irani, C. DeLisi, M. Chiari, and M. S. Unlu, Biosens. Bioelectron. **25,** 1789 (2010).
17. E. Ozkumur, A. Yalcin, M. Cretich, C. A. Lopez, D. A. Bergstein, B. B. Goldberg, M. Chiari, and M. S. Unlu, Biosens. Bioelectron. **25,** 167 (2009).
18. C. Joo, E. Ozkumur, M. S. Unlu, and J. F. Boer, Biosens. Bioelectron. **25,** 275 (2009).
19. G. G. Daaboul, R. S. Vedula, S. Ahn, C. A. Lopez, A. Reddington, E. Ozkumur, and M. S. Unlu, Biosens. Bioelectron. **26,** 2221 (2011).
20. T. Wang, Q. Li, X. Li, S. Zhao, Y. Lu, and G. Huang, Opt. Lett. **38,** 1524 (2013).